Journal of the Korean Nuclear Society
Volume 26, Number 3, September 1994

Study on Radionuclide Migration Modelling for a Single Fracture in Geologic Medium : Characteristics of Hydrodynamic Dispersion Diffusion Model and Channeling Dispersion Diffusion Model

D.K. Keum, W.J. Cho, P.S. Hahn, and H.H. Park
Korea Atomic Energy Research Institute
(Received February 14, 1994)

단일균열 핵종이동모델에 관한 연구 —수리분산확산모델과 국부통로확산모델의 특성—

금동권 · 조원진 · 한필수 · 박헌휘
한국원자력연구소
(1994. 2. 14 접수)

Abstract

Validation study of two radionuclide migration models for single fracture developed in geologic medium, the hydrodynamic dispersion diffusion model(HDDM) and the channeling dispersion diffusion model(CDDM), was studied by migration experiments of tracers through an artificial granite fracture on the labolatory scale. The tracers used were Uranine and Sodium lignosulfonate known as nonsorbing material. The flow rate ranged 0.4 to 1.5 cc/min. Related parameters for the models were estimated by optimization technique. Theoretical breakthrough curves with experimental data were compared.

In the experiment, it was deduced that the surface sorption for both tracers did not play an important role while the diffusion of Uranine into the rock matrix turned out to be an important mass transfer mechanism. The parameter characterizing the rock matrix diffusion of each model agreed well. The simulated results showed that the amount of flow rate could not tell the CDDM from the HDDM quantitatively. On the other hand, the variation of fracture length gave influence on the two models in a different degree. The dispersivity of breakthrough curve of the CDDM was more amplified than that of the CDDM when the fracture length was increased. A good agreement between the models and experimental data gave a confirmation that both models were very useful in predicting the migration system through a single fracture.

요 약

실험실 규모의 인공균열 추적자 이동실험을 통해 지하매질의 단일균열을 위한 핵종이동 모델중 수리분산확산모델 및 국부통로확산모델의 타당성이 연구되었다. 사용된 추적자는 비수착성으로 알려진 우라

닌과 소디움 리그노설포네이트 이었으며 적용유량은 0.4에서 1.5cc /min의 범위였다. 최적화법으로 모델들의 관련 매개변수들을 구하였으며 모델과 실험결과를 비교하였다.

실험에서 우라닌은 암석내로의 확산이 중요한 인자임을 보여주었고, 두 물질 모두 균열 표면에서의 수착은 중요하게 작용하지 않았다. 두 모델의 암석확산을 나타내는 매개변수값들은 서로 잘 일치하였다. 모사결과에 따르면 유량변화시 두 모델은 정량적으로 같은 결과를 주었으나, 균열길이는 다른 크기로 두 모델에 영향을 주었다. 즉, 균열길이가 커짐에 따라 국부통로확산모델의 파과곡선 퍼짐성(dispersivity)이 수리분산확산모델의 파과곡선 퍼짐성보다 증가하였다. 실험과 모델들의 일치는 위 두모델들이 단일 균열 시스템을 해석하는데 매우 유용함을 입증하였다.

1. Background

Studies on the radionuclide transport through underground rock fracture have been carried out in many countries with radioactive waste disposal program.

Radionuclides leached from waste forms are released into geologic environment with the groundwater flowing around the waste disposal facility. To analyze and predict such migration phenomena, well characterized data are required to reduce the uncertainty of the system. Actually, fractures in rock are entangled in complex structure each other and flow is fairly uneven and irregular. However, it can be conceptually simplified to the flow system through a single fracture. Uncertainty caused by postulating the inaccurate actual system can be more severe than the errors by interpreting postulated phenomena. From such a point of view, an experiment through a single fracture under the well defined condition can be very valuable and practical in order to study the radionuclide transport phenomena in the underground rock. For example, Neretnieks and his co-workers[1] applied single fracture system to the safety assessment of the SFR, the Swedish repository facility for low-and medium level radioactive waste.

Present work is aimed at comprehending characterization of the radionuclide migration system, and looking into validation of two models for a single fracture, the hydrodynamic dispersion diffusion model(HDDM) and the channeling dispersion diffusion model(CDDM), using artificial single fracture experiments on the laboratory scale.

2. Models

Radionuclide transport through rock fracture is influenced by, a number of effects such as dispersion by molecular and eddy diffusion or velocity difference along pathways, physical and chemical interaction between radionuclides and rock matrix and so on. The representative models for a single fracture are the hydrodynamic dispersion diffusion model (HDDM) and the channeling dispersion diffusion model(CDDM). The HDDM(see Fig. 1a) assumes that the radionuclide moves with the underground water flowing between parallel walls with the constant fracture width, and that the molecular or eddy diffusion of fluid causes the dispersion. In the CDDM (see Fig. 1b) it is assumed that fracture consists of a set of parallel apertures that are different in width and unconnected each other, and the dispersion is caused by the velocity differences due to the different aperture size or water flow resistance.

2.1. Hydrodynamic Dispersion Diffusion Model(HDDM)

This model considers the five phenomena as follows: (a) advective transport, (b) longitudinal dispersion, (c) sorption onto surface of fracture, (d) diffusion into rock matrix, and (e) sorption within rock matrix. It is assumed that all sorption reactions are

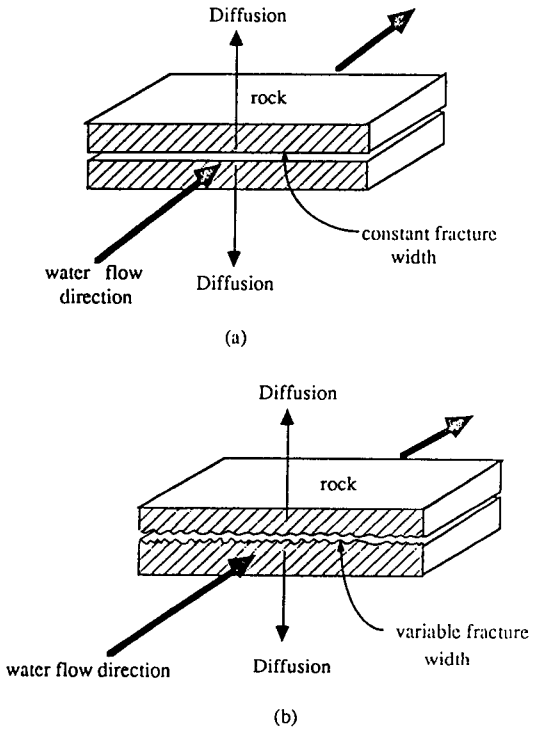

Fig. 1. Conceptual Diagrams of (a) Hydrodynamic and (b) Channeling Dispersion Diffusion Model

reversible and instantaneous, and there exists the local linear equlibrium. Then the differential transport equation of the tracer in the fracture is expressed as:

$$\frac{\partial C_f}{\partial t} + \frac{U_f}{R_{a,\mu}} \frac{\partial C_f}{\partial x} = \frac{D_L}{R_{a,\mu}} \frac{\partial^2 C_f}{\partial x^2} + \frac{2}{\mu} \frac{D_e}{R_{a,\mu}} \frac{\partial C_p}{\partial z} \Big|_{z=0} \quad (1)$$

where

μ : fracture width, cm

C_f : concentration in the liquid in the fracture, mol/cm^3

C_p : concentration in the liquid in the pore, mol/cm^3

U_f : water velocity, cm/min

D_L : dispersion coefficient, cm^2/min

t : time, min

x : distance in the direction of flow, cm

z : distance into rock matrix, cm

$R_{a,\mu}$ is the surface retardation factor defined as:

$$R_{a,\mu} = 1 + \frac{2}{\mu} K_a \quad (2)$$

where K_a is surface distribution coefficient. Also, for the rock matrix

$$\frac{\partial C_p}{\partial t} = \frac{D_e}{K_d \rho_p} \frac{\partial^2 C_p}{\partial z^2} \quad (3)$$

where D_e is effective diffusion coefficient and K_d is bulk distribution coefficient and is related to solid distribution coefficient, K'_d by

$$K_d \rho_p = \varepsilon_p + K'_d \rho_p \quad (4)$$

where

ε_p : porosity of rock matrix

ρ_p : density of rock matrix, g/cm^3

Initial and boundary conditions are

$$I.C.: \quad C_f(0,x) = C_p(0,x,z) = 0 \quad \text{for } all\ x,\ z \quad (5)$$

$$\begin{aligned} B.C: \quad & C_f(t,0) = C_o && t > 0 \\ & C_f(t,\infty) = 0 && t > 0 \\ & C_p(t,x,\mu/2) = C_f(t,x) && t>0,\ x>0 \\ & C_p(t,x,\infty) = 0 && t>0,\ x>0 \end{aligned} \quad (6)$$

The solution of Eq. (1) subject to Eqs. (5) and (6) is the special form of the general solution derived originally by Tang et. al. [2]. Afterward, Moreno et. al. [3] utilized the solution as:

$$\frac{C_f(x,t)}{C_o} = \frac{2}{\sqrt{\pi}} \exp\left(\frac{Pe}{2}\right) \int_l^\infty \exp\left(-\xi^2 - \frac{Pe^2}{16\xi^2}\right) erfc\left(\frac{\frac{Pet_o}{8a\xi^2}}{t - \sqrt{\frac{Pet_o}{4\xi^2}}}\right) d\xi \quad (7)$$

where

$$l = \sqrt{Pet_o/4t}$$

$$Pe = U_f x / D_L$$

$$t_w = x/U_f$$

$$t_o = R_{a,\mu} \cdot t_w = \left(1 + \frac{2}{\mu} K_a\right) \cdot t_w$$

$$\alpha = \mu R_{a,\mu}/2\sqrt{D_a K_d \rho_p} = \mu(1+\frac{2}{\mu}K_a)/2\sqrt{D_e K_d \rho_p}$$

2.2. Channeling Dispersion Diffusion Model(CDDM)

This model considers the channeling dispersion instead of the longitudinal dispersion of the HDDM. It is assumed that the hydrodynamic dispersion in each channel is regarded as negligible compared to the channel dispersion. Then the transport equation for a channel with the width, δ is written as:

$$\frac{\partial C_f'}{\partial t} + \frac{U_f}{R_{a,\delta}} \cdot \frac{\partial C_f'}{\partial x} = \frac{2}{\delta} \cdot \frac{D_e}{R_{a,\delta}} \cdot \frac{\partial C_p}{\partial Z}\Big|_{z=0} \quad (8)$$

The diffusion equation into rock matrix is the same as the Eq. (3). The initial and boundary conditions are respectively given as follows:

$$I.C.: \; C_f'(0,x) = C_p(0,x,z) = 0 \quad \text{for all} \quad x \;, z \quad (9)$$

$$\begin{aligned} B.C.: \; & C_f'(t,0) = 0 && t>0 \\ & C_p(t,x,\delta/2) = C_f'(t,x) && t>0\,,\; x>0 \\ & C_p(t,x,\infty) = 0 && t>0\,,\; x>0 \end{aligned} \quad (10)$$

With the initial and boundary conditions given, the concentration at exit of a channel is obtained as the following [4]:

$$\frac{C_f'}{C_o} = erfc\left(\frac{\beta \cdot \overline{t_w}}{\delta \cdot \sqrt{(t-t_o)}}\right), \quad t<t_o$$

$$= 0, \quad t>t_o \quad (11)$$

where

$$R_{a,\delta} = 1+\frac{2}{\delta} \cdot K_a$$

$$\overline{t_w} = \frac{x}{U_f}$$

$$t_o = R_{a,\delta} \cdot \overline{t_w} = (1+\frac{2}{\delta} \cdot K_a) \cdot \overline{t_w}$$

$$\beta = \sqrt{D_e \cdot K_d \cdot \rho_p}$$

When the flows from all channels are perfectly mixed at the outlet of the fracture, the average concentration of total flow can be expressed as:

$$\frac{C_f(t)}{C_o} = \frac{\int_0^\infty f(\delta)Q(\delta)C_f'(\delta,t)d\delta}{\int_0^\infty f(\delta)Q(\delta)d\delta} \quad (12)$$

where $f(\delta)$ is an arbitrary fissure width distribution function and $Q(\delta)$ is the flow rate that is proportional to the width to the third power. In the present work, the lognormal distribution was applied [3, 5]. The gamma distribution or discrete distibution also can be applied. The lognormal distribution has the following form:

$$f(\delta) = \frac{1}{\sqrt{2\pi} \cdot \delta \cdot \sigma} \exp\left[-\frac{1}{2}\left(\frac{\ln(\delta/\mu')}{\sigma}\right)^2\right] \quad (13)$$

where

$$\overline{\mu} = \mu' \exp\left(\frac{\sigma^2}{2}\right)$$

where $\overline{\mu}$ is average aperture value on linear scale, and μ' and σ are respectively average aperture value and standard deviation on logarithm scale.

The solutions of the above two models have four parameters respectively that are Pe, K_a, μ, α for the HDDM and σ, K_a, $\overline{\mu}$, β for the CDDM. Of them, Pe, σ, μ, and $\overline{\mu}$ are calculated from experimental curves obtained under conditions of non-sorption and non-diffusion. The K_a for surface sorption or the lumped parameters, α and β, is determined from tracer experiments with the surface sorption or the rock matrix diffusion.

On the other hand, although the physical idea of the hydrodynamic dispersion and the channeling dispersion are different, the dispersivity of the breakthrough curve from both models is quantitatively related each other. Neretnieks[5] and Moreno et. al: [3] have found, by analytical method and curve fitting method, respectively, that the following relation between Pe and σ is possible if there is neither sorption nor rock matrix diffusion:

$$\Delta\sigma_t^2 / \overline{t^2} = \frac{2}{Pe} = \exp(4\sigma^2) - 1 \quad (14)$$

where $\bar{t}$ is the mean residence time and σ_t the second statistical central moment for a response curve. The ratio, $\Delta_t^2\sqrt{t^2}$, accounts for the dispersivity of the response curve. Whether the calculated Pe and σ satisfy the relation or not may be used as a criterion for the verification of the calculation procedure.

3. Experimental

The tracers used were Uranine (molecular weight: 376) and Sodium lignosulfonate (NaLS, molecular weight: 24,000) known as a non-sorbing material, and the solution with the initial concentration of 10^{-8} *mole/cm*^{3} was prepared using distilled water.

An artificial fracture was made of two granite blocks, 10cm in width(x_b) and 40cm in length(x_l). The outer surfaces of the granite blocks were coated by urethane lacquer to prevent water loss by vaporization. The artificial fracture rock was fixed between two end plates made from acryl plate and teflon sheet. At the central part of each end plate a flow channel of (10×0.2)cm was pierced.

Figure 2 shows the schematic diagram of the experimental system. The fracture block was laid to be parellel with the ground. Before experiment, distilled water was pumped into fracture in order to saturate the rock with water. Step injection of the solution was made using the three way valve installed in front of the solution pump. The flow rate(F_R) ranged from 0.4 to 1.5 cm^3/min. The effluent at the outlet of the fracture was collected using fraction collector. The concentration of the collected sample was measured by spectrophotometer at 490 μm adsorption wavelength for Uranine and 290 μm for NaLS

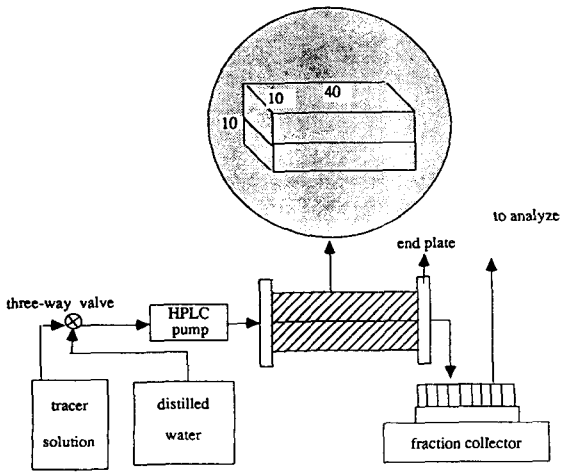

Fig. 2. Schematic Diagram of Experimental Appartus

4. Results and Discussions

4.1. Experimental Results

Typical breakthrough curves for NaLS and Uranine are shown in Figure 3. Uranine curves have a long tail. This may result from a number of effects such as existence of water stagnant zone, surface sorption, and rock matrix diffusion. If the existence of stagnant zone is dominant, the same phenomenon should be observed for NaLS curves. As shown in the Figure 3, the NaLS curves do not show the long tail and so water stagnant zone may not be the cause. Since both materials are regarded as nonsorbing, the sorption will not become the contributor, either. The rock matrix diffusion is likely to be the major contributor to the tailing effect. It is suggested that NaLS with large molecule be excluded from rock matrix while Uranine with small molecule be freely diffused into it.

The system parameters, Pe, μ for the HDDM, and σ, $\bar{\mu}$ for the CDDM, were calculated by the Marquardt' Besolve algorithm [6] using NaLS experiment data. Caculated values respectively ranged 10 to 14 for Pe, and 0.19 to 0.22 for σ according to the flow rate. Those values of both models are summerized in Table 1 and 2. The Pe should be a constant irrespective of the water velocity in the region where the dispersion coefficient is only proportional to the water velocity. The present result shows only a small deviation of Pe and supports the fact. The fracture

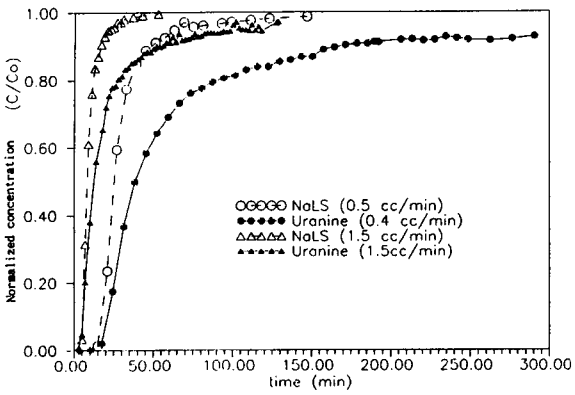

Fig. 3. Experimental Breakthrough Curves With NaLS and Uranine (A Number in Parenthesis Indicates Flow rate)

width, μ and $\bar{\mu}$, determined from average retention time are equal to around 0.035cm on an average for both models. In order to verify the calculation procedure, the relation between Pe and σ, Eq. (14), was also tested. As shown in Tables 1 and 2, the Pe values for HDDM and the σ for CDDM satisfy the Eq. (14) well.

The parameters for Uranine were also caculated by curve fitting method. In the calculation, the used values of Pe and σ were, 12 and 0.2 respectively, which were averaged values determined from experiment with NaLS. It should be indicated that the Pe was obtained when the fracture length was only 40cm. The value obtained for a certain fracture length could not be used for the case of different fracture distance. However, the Pe at a fracture

Table 1. Calculated Parameters for NaLS Fitted into the HDDM

Tracer	F_R	P_e	t_w	$\mu=\frac{F_R t_w}{\bar{x}_f \bar{x}_w}$	$U_f=\frac{F_R}{\mu x_b}$	$D_L=\frac{U_{fx}}{P_e}$	ϕ^*
	(cm³/min)		*(min)*	*(cm)*	*(cm/min)*	*(cm²/min)*	
NaLs	1.5	10.0	9.3	0.035	4.3	17.1	0.02
NaLs	1.0	12.3	14.5	0.036	2.8	9.0	0.03
NaLs	0.5	13.8	28.0	0.035	1.4	4.1	0.03
average		12.0		0.035			

$^*\phi = \frac{1}{N}\sum_{n=1}^{N}(C_f^{exp} - C_f^{the})^2/C_0^2$, N = number of experimental data

Table 2. Calculated Parameters for NaLS Fitted into the CDDM

Tracer	F_R	σ	$\bar{t}_w$	$\mu=\frac{F_R \bar{t}_w}{\bar{x}_f \bar{x}_w}$	$P_e=\frac{2}{e^{4\sigma^2}-1}$	ϕ^*
	(cm³/min)		*(min)*	*(cm)*		
NaLs	1.5	0.215	9.3	0.035	9.8	0.02
NaLs	1.0	0.195	14.5	0.036	12.2	0.03
NaLs	0.5	0.185	28.0	0.035	13.6	0.03
average		0.200		0.035		

$^*\phi = \frac{1}{N}\sum_{n=1}^{N}(C_f^{exp} - C_f^{the})^2/C_0^2$, *N = number of experimental data*

length can be predicted by a simple proportional relationship. Tables 3 and 4 show the surface sorption coefficient values, K_a, and the lumped parameter values, $D_e K_d \rho_t$, for the HDDM and the CDDM respectively. The $D_e K_d \rho_t$ does not show any particular trend with flow rates. On the whole, the $D_e K_d \rho_t$ from both models agrees well within the same factor. The very small difference of $D_e K_d \rho_t$ between the two cases considering only the rock matrix diffusion and considering both rock matrix diffusion and surface sorption means that surface sorption does not play an important role.

4.2. Simulation Results

Gaussian quadrature was applied to solve Eqs. (7) and (12). This method [7] combines the Gauss-Legendre quadrature with the Gauss-Lagurre quadrature according to the integral interval. The numerical scheme is simple without loss of accuracy and especially effective when the upper integral limit goes to infinite.

Figure 4 shows the effect of Pe on the breakthrough curves of the HDDM. The curves are more sharpened with the increase of Pe. Since the Pe accounts for relative importance of dipersion compared with advection, greater value of Pe corresponds to less dispersion effect. In Figure 5 the effect of σ on the breakthrough curves of the CDDM is given. The dispersivity increases with the standard deviation(σ) because the larger σ gives the wider water velocity distribution.

Figure 6 (a) and (b) respectively shows the comparison between the curves predicted by two models when the fluid velocity and the fracture length are varied. The predicted curves with a half velocity of the reference case as shown in Figure 6(a) are independent of the selected model. Usually, the hydrodynamic dispersion coefficient, D_L, is uniquely proportional to water velocity [8]. It indicates the

Table 3. Calculated Parameters for Uranine Fitted into the HDDM for Three Mechanisms

flow frat	Peclet number		rock diffusion			surface sorption			rock diffusion and surface sorption		
	(Pe)	t_w	K_a	$D_e K_d \rho_p \cdot 10^6$	ϕ^*	K_a	$D_e K_d \rho_p$	ϕ^*	K_a	$D_e K_d \rho_p \cdot 10^6$	ϕ^*
1.5		9.33	–	5.5	0.03	0.007	–	0.49	0.0016	4.9	0.03
1.0		14.00	–	9.7	0.03	0.018	–	1.16	−0.0007	11.0	0.03
0.7	12	20.00	–	2.0	0.01	0.007	–	0.45	−0.0007	2.3	0.01
0.4		35.00	–	1.1	0.02	0.007	–	0.52	−0.0014	1.6	0.01

$^*\phi = \frac{1}{N}\sum_{n=1}^{N}(C_f^{exp} - C_f^{the})^2/C_0^2$, N = number of experimental data

Table 4. Calculated Parameters for Uranine Fitted into the CDDM for Three Mechanisms

flow frat			rock diffusion			surface sorption			rock diffusion and surface sorption		
	σ	t_w	K_a	$D_e K_d \rho_p \cdot 10^6$	ϕ^*	K_a	$D_e K_d \rho_p$	ϕ^*	K_a	$D_e K_d \rho_p \cdot 10^6$	ϕ^*
1.5		9.33	–	5.6	0.04	0.016	–	0.36	0.0035	4.4	0.02
1.0		14.00	–	10.6	0.03	0.026	–	0.78	0.0015	9.6	0.02
0.7	0.2	20.00	–	2.0	0.01	0.009	–	0.37	0.0003	2.0	0.01
0.4		35.00	–	1.2	0.01	0.006	–	0.46	0.0	1.2	0.01

$^*\phi = \frac{1}{N}\sum_{n=1}^{N}(C_f^{exp} - C_f^{the})^2/C_0^2$, N = number of experimental data

value of Pe representing the measure of the dispersivity is maintained as constant irrespective of water velocity. Also, in our experimental result it showed that the Pe was nearly independent of the flow rate. In the case of CDDM, the dispersivity is only a function of the standard deviation of the aperture width distribution. When the rock matrix diffusion is considered, there is a slight difference between the two models. This difference is attributed to not the water velocity variation but the invalidity of Eq. (14) when the rock matrix diffusion is accounted for. On the other hand, the variation of fracture length leads to a different situation(see Fig. 6b). At the same water velocity, the predicted curve by the CDDM for a doubled fracture length of the reference case is more dispersive than that by the HDDM. In the HDDM, the dispersivity is inversely proportional to the fracture length. However, the dispersivity in the CDDM is independent of fluid velocity as well as of fracture length as shown in Eq. (14). As a result, the curve from the CDDM is apparently more dispersive than that from the HDDM. This difference is further amplified with the increase of the fracture length. If rock matrix diffusion is taken into account, then the CDDM predicts much faster release and higher concentration at the early part of the break-

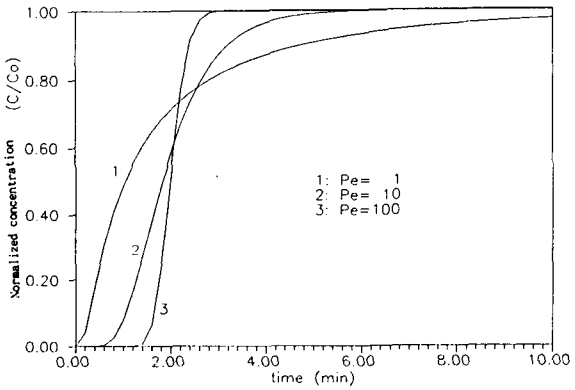

Fig. 4. Effect of Peclet Number on the Predicted Curves of the HDDM (t_w=2 min, K_a=0, $\alpha=\infty$)

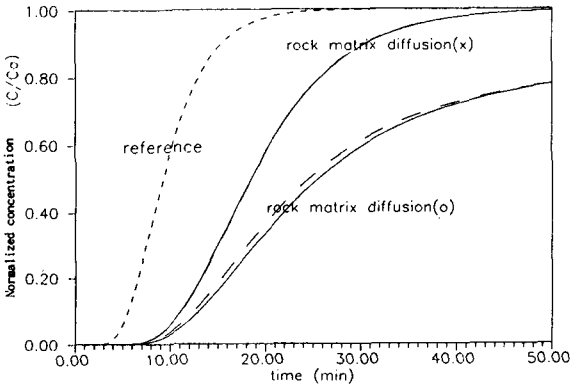

Fig. 6(a). Predicted Curves by HDDM(—) and CDDM(– –) with a Half Velocity of the Reference Case

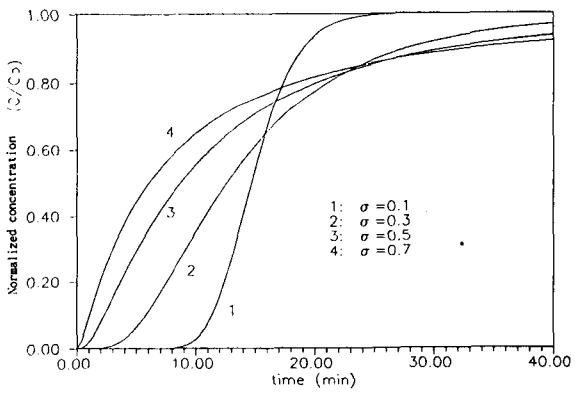

Fig. 5. Effect of σ on Predicted Curves of the CDDM (t_w=15 min, K_a=0, β=0)

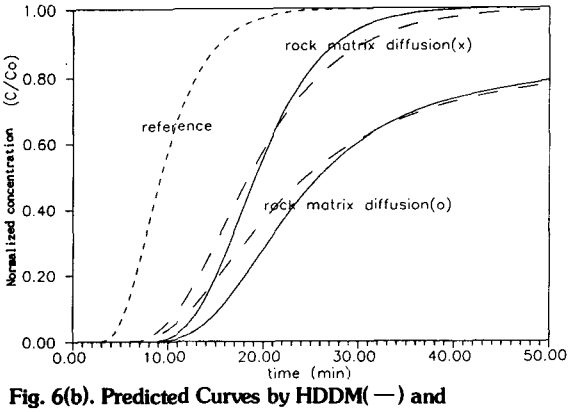

Fig. 6(b). Predicted Curves by HDDM(—) and CDDM(– –) with a Doubled Distance of the Reference Case

through curve than that of the HDDM while both approaches show a similar trend at the trail part. This is due to the facts that the dispersion is dominant at the early stage of mass transfer and the rock matrix diffusion contributes more to the mass balance at the later time.

4.3. Comparison Between Models and Experimental Data

Figure 7 shows a comparision between experimental result with NaLS and the predictions by two models, the HDDM and the CDDM. It gives a good agreement between experimental data and modelling results. The small trail from experimental data is believed to be caused by backmixing around the end plate.

The experimental result with the Uranine tracer is compared with the model predictions by both approaches in Figures 8 and 9. Considering only the surface sorption, the predictions from both models deviate very much from the experimental data. However, if the rock matrix diffusion is taken into account, both models can predict the experimental data with excellent accuracy including the trail zone in particular. From this it can be concluded that the rock matrix diffusion brings about the tailing effect in the experimental curve with Uranine.

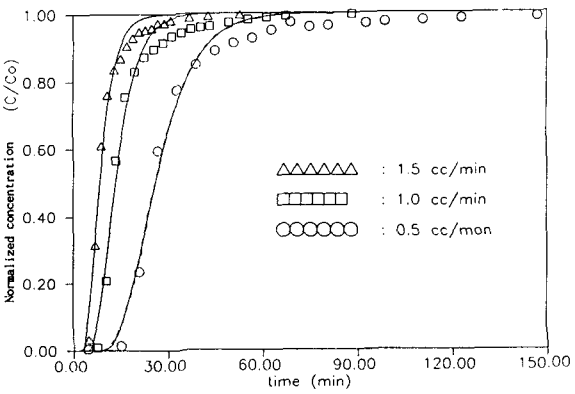

Fig. 7. Comparison of Experimental Data with NaLS with CDDM(—) and HDDM(---)

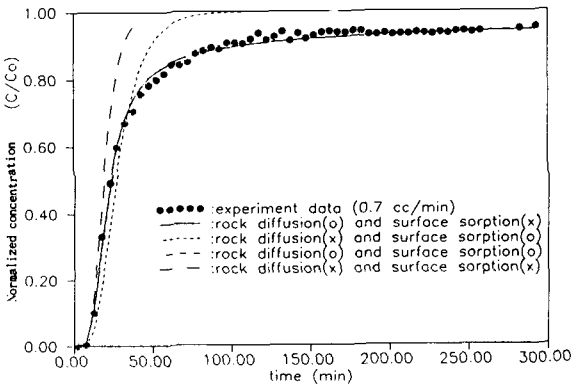

Fig. 8. Comparison of Experimental Data with Uranine with HDDM

5. Conclusion

Laboratory scale experiments with an artificial single fracture have been carried out to comprehend and to analyze the radionuclide migration and to establish a validation of model predictions. This work dealed with two models for a single fracture, the hydrodynamic dispersion diffusion model and the channeling dispersion diffusion model. The parameters representing the physical and chemical mechanisms were determined using the Marquardt' Besolve algorithm.

In the experiment Uranine diffused into rock

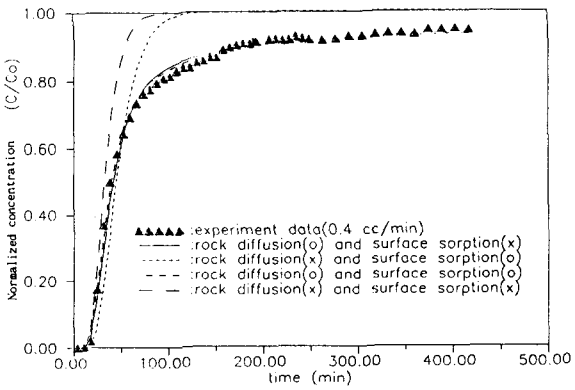

Fig. 9. Comparison of Experimental Data with Uranine with CDDM

matrix, and the surface sorption did not play an important role for both tracers. The parameter characterizing the rock matrix diffusion agreed well between the two models. The simulated results showed that the selected model was independent of the amount of flow rate while the length of fracture had influence on the model predictions. The dispersivity of breakthrough curve of the CDDM was relatively greater than that of the HDDM when the fracture length was larger than the reference case. This trend is even more amplified with the increase of the fracture length

Both models excellently fitted the experimental data and predicted nearly the same parameter value for the same experimental data. However, it should be reminded that the CDDM will give the faster release and the higher concentration than the HDDM when the prediction is extrapolated to a larger scale.

This result can be utilized to support the validation of migration modelling for the safety assessment of the repository. The subsequent work will focus on the migration experiments with sorbing radionuclides to study the effects of surface sorption on the nuclide migration.

References

1. I. Neretnieks, S. Arve, L. Moreno, A. Rasmuson, and M. Zhu, Degradation of concrete and transport of radionuclides from SFR repository for low- and intermediate-level nuclear waste, SFR 87-11, 1988.
2. D.H. Tang, E.O. Frind, and E.A. Sudicky, Contaminant transport in fractured porous media: An analytical solution for a single fracture,Water Resour. Res., 17(3), 555-568, 1981
3. L. Moreno, I. Neretnieks, and T. Erikson, Analysis of some laboratory tracer runs in natural fissures, Water Resour. Res., 21(7), 951-958, 1985
4. H.S. Carslaw, and J.C. Jaeger, Conduction of heat in solids, 2nd ed., p. 396, Oxford University Press, 1959
5. I. Neretnieks, A note on fracture flow dispersion mechanism in the ground, Water Resour. Res., 19 (2), 364-370, 1983
6. J.L. Kuester, and J.H. Mize, Optimization techniques with FORTRAN, McGraw-Hill Book Company, 1973
7. B. Carnahan, H.A. Luther, and J.O. Wilkes, Applied Numerical Methods, John Wiley & Sons, Inc., 1969
8. J. Bear, Hydrodynamic dispersion: Flow through porous media, edited by R.J.M. de Wiest, Academic, New York, 1969